Desalination and Water Treatment
www.deswater.com

doi: 10.5004/dwt.2019.23973

153 (2019) 216–225
June

Column adsorption studies on copper(II) ion removal from aqueous solution using natural biogenic iron oxide

Brij Kishor, Nekram Rawal*

Department of Civil Engineering, Motilal Nehru National Institute of Technology, Allahabad 211004, India, email: brijkishorgood@gmail.com (B. Kishor), Tel. +91- 9336146896, email: nek_friend@rediffmail.com (N. Rawal)

Received 24 September 2018; Accepted 17 February 2019

ABSTRACT

Over the past years, the tremendous increase of toxic pollutants like heavy metals from industrial wastes have been spoiled water bodies and groundwater, it caused deterioration of drinking water quality. Therefore, it is necessary to remove copper (Cu) metal ion from wastewater up to the permissible limits. This can be achieved by adsorption on low cost naturally occurring biogenic iron oxides (Banded Iron Formation form) used as the low cost adsorbent. In this work, the experiments were performed on laboratory scale fixed-bed column to remove Cu(II) ion from aqueous solution on natural biogenic iron oxide material. The performance of column was investigated by varying flow rate, bed depth and inlet metal ion concentration. The maximum breakthrough time was obtained by increasing the bed depth and by decreasing the flow rate. The adsorption capacity was found to be 1669.7 mg/L by the bed depth service time model and best fitted with high correlation coefficient value with experimental data, suitable to estimate the bed depth and service time of the column. The experimental results have proven to be viable and sustainable adsorbent for copper(II) metal ion removal from water and wastewaters.

Keywords: Copper(II); Banded iron formation; Adsorption; Fixed-bed column; Column adsorption models

1. Introduction

Over the past years, the tremendous increase of toxic pollutants like heavy metals from industrial wastes have spoiled water bodies and groundwater, it caused deterioration of drinking water quality. The industries like mining, metal cleaning and plating facilities, fertilizer industries, tanneries, batteries, paper industries and pesticides galvanizing plants, electronic device manufacturing industries and many more released the waste containing the considerable amount of toxic and hazardous heavy metal [1,2]. Among all, the particular attention has been given to toxic heavy copper (Cu) metal ion is consider for this study. The copper is an important engineering material of choice for technologies and having the wide industrial application [3]. It is the prime nutrient in small amount but at higher concentration poses the serious threat to mankind as well as plants and algae. Copper has properties of biological magnification, non-biodegradability and long-time persistent in the environment that cause the adverse effect on the environment and health. The Cu metal enters into the human through polluted water, air, and foods but beyond the permissible limit causes harmful effects on health. The excessive intake of Cu may cause gastrointestinal disorders, hemolysis, hepatotoxic and nephrotoxic effects. Copper toxicity leads to serve mucosal irritation, widespread capillary damage, renal damage and central nervous system irritation followed by depression [4]. Therefore, it is essential to be removed Cu(II) ion from water and wastewater for health and environment protection. The various methods are available for the removal of heavy metals like Cu(II) ion from water and wastewater namely: ion exchange, chemical precipitation, solvent extraction, coagulation and membrane processes, but most of these methods are hardly handle, and are very costly [5–8]. The biomasses derived from plants are non-toxic, abundant,

*Corresponding author.

eco-friendly, and inexpensive an efficient adsorbent for adsorption of heavy metal ions onto the carbonic substances [9,10].

The adsorption process can be a reliable method for the removal of Cu(II) ion [11]. A number of low-cost adsorbents have been successfully used for removal of Cu(II) ion from water and wastewater [12,13]. The various forms of iron oxide adsorbent materials have been studied for the removal of Cu(II) metal ion. The hematite nanoparticles used for removal of Cu(II) ion and studied the effect of sorbent concentration, pH, temperature etc. [14]. The iron nanoparticles (Fe_2O_3), zerovalent iron nanoparticles (nZVI) and nickel and copper ferrite ($NiFe_2O_4$ and $CuFe_2O_4$) used for Cu(II) ion removal from aqueous solution by electrochemical methods [15–17].

The naturally occurring biogenic iron oxides of banded iron formation (BIF form) from the mines is one of the low-cost adsorbents. Researchers reported that the variety of natural biogenic iron oxides (BIF) form adsorbent, showed efficient removal of heavy metal ion from water and wastewater. The toxic water-soluble organic dyes were removed by a natural biogenic iron oxide material [18–21]. The *Leptothrix ochracea* dominated natural iron oxide is used for Cu(II) ion removal from solution [22]. The phosphorus and arsenic are also removed through bioremediation methods by fluidized raw dolomite bed [23].

In history, the Archean and Proterozoic eras known for the deposition of banded iron formation in the Earth. These are large deposits of iron-rich BIF form ores contains 25% to 35% iron and deposited in billion of tons in natural sedimentary rocks of Precambrian age and available all around the world [24,25]. Natural biogenic iron oxides (BIF form) are produced by weathering, metabolic activity or series of bacterial metabolic activities, passive reaction, and internal biomineralization processes. The metabolic activity of acidophilic and neutrophilic iron-oxidizing bacteria helps in the oxidation of Fe(II) to Fe(III) under the oxic condition to form biogenic iron oxides [23,26,27]. The various forms of biogenic iron oxides are available on the earth's environment in the wetland, lakes, rivers (freshwater and marine), soil and also in mines [28–30]. In this work, the natural biogenic iron oxide (BIF form) material used as an adsorbent for the removal of Cu(II) ion by adsorption technique from aqueous solution and the experiments were conducted to the laboratory scale fixed-bed column. To examine the performance of the natural biogenic iron oxide (BIF form) material adsorbents for removal of Cu(II) ion for varying process design parameters, viz. bed depth, flow rate, and inlet metal ion concentration in a fixed bed column. The breakthrough curves were analyzed using bed-depth and service time (BDST), mass transfer, Yoon-Nelson, Thomas and Adam-Bohart, models.

2. Materials and methods

2.1. Reagents and stock solution

The analytical grade chemicals were used for the preparation of all the reagents in the study. The stock solution of Cu(II) ion was prepared as per standard methods APHA, 2012. All the solutions were prepared in double distilled water.

2.2. Natural biogenic iron oxide (BIF form) adsorbent media

The Dalli Rajhara in Durg (India) is located at 20.58°N, 81.08°E. The natural biogenic iron oxide (Fe_2O_3) in BIF form (iron ore) was discovered in 1900 at Dalli-Rajhara. This place is known as the home of iron ore captive mines for the integrated steel plant in India. The iron ore obtained from mines was washed with distilled water to remove the soil particles and crushed into powdered form. The media was oven dried at 105°C for 3–4 h, then passed through the geometric sieve of 300, 150 and 75 µm size for different particle size. The natural biogenic iron oxide (BIF form) particles of different sizes were stored in plastic jars for column experiment [31].

2.3. Preparation of aqueous solution

The standard methods, APHA (2012) [32] follow for the preparation of aqueous Cu(II) ion solution for this studies. The 200 mg of polished electrolytic copper wire or foil was inserted into 250 mL conical flask, then 5 mL concentration HNO_3 solution and 10 mL water ware added in the same conical flask. After the reaction, warm gently to complete dissolution of the copper and then boil to expel oxides of nitrogen. All precautions must be taken to avoid loss of copper from solution. The solution was cooled down and again 50 mL water was added. The whole solution was again transferred quantitatively to a 1 L volumetric flask and diluted to the mark with water; 1 mL = 200 µg Cu.

The Bathocuproine methods are used for the determination of the concentration of Cu(II) ion as per standard methods, APHA (2012). The UV/VIS spectrophotometer (Model: Lab India UV 3000+, Lab India Analytical Instruments Pvt. Ltd) used for measurement of absorbance at 484 nm wavelengths. The digital pH meter (Model: Cyber Scan pH 510/Ion 510, Eutech Instruments, Singapore) is used for pH measurement.

2.4. Characterization of adsorbents

A small portion of natural biogenic iron oxides (BIF form) media was taken for morphological characterization. The energy dispersive x-ray spectroscopy (EDS) analysis was carried out for finding the normalized element composition (by weight percentage) percentage and elemental spectra of adsorbent media before and after adsorption. It was analyzed by EDS instrument (Model: FEI Quanta 200F with Oxford-EDS system IE 250 X Max 80, Netherlands). The EDS was analyzed to identify their relative proportions (by weight and atomic percentage) present in natural biogenic iron oxide (BIF form) adsorbent before and after Cu(II) ion adsorption.

The x-ray diffraction (XRD) analysis of adsorbent was carried out to find the types of minerals oxide present in the sample. The x-ray diffraction was obtained by powder or thin film X-ray diffraction system with low-temperature attachment PANalytical X'pert PRO (Model: 'X' pert pro mrd Panalytical) with 'X' pert data collector, PW 3050/65 High-resolution goniometer. The diffraction data were collected from diffractometer at these operating condition i.e. wide angle goniometer operated at 40 kv and 40 mA, start position (2θ°) 100 , end position (2θ°) 800, step size (2θ°) 0.02, scan step time 1 s (s) and radiation Cu-Kα.

The Fourier transform infrared (FTIR) spectroscopy of BIF form adsorbent before and after Cu(II) ion adsorption were carried out to obtain the spectrum in the range of 4000 to 400 cm^{-1}. The functional groups that are present in the sample are represented in the form of absorption bands (cm^{-1}). The FTIR were analyzed at room temperature using KBr pellet technique in the range of 400–4000 cm^{-1} by FTIR spectrometer (Model: Perkin Elmer Spectrum BX FTIR Systems USA). The BIF particles of 75 µm size mixed with KBr (IR Spectroscopic Grade) in the ratio of 2: 200 or 20% (weight). The composition was carefully mixed homogeneity, without any change of the surface or destroying the BIF particle.

2.5. Column study

The column experiments were conducted under the varying bed depth, flow rates and inlet metal ion concentration for the study of breakthrough time required for the uptake of Cu(II) ion by natural biogenic iron oxide (BIF form) material. Three glass columns, 3 cm identical internal diameter each with different media depths of 10, 20 and 30 cm were used to generate requisite data for adsorption column models. The packed adsorbent beds were supported by 3 cm glasswool at the bottom of the columns. The influent flow rate was maintained by the peristaltic pump (Model-PP10-EX) in different bed depths and concentration studies, except for flow variation study. The three flow rate i.e. 0.283, 0.565 and 0.848 $m^3/m^2/h$ used in this study. The effluent samples were collected at fixed time intervals and were analyzed for residual Cu(II) ion concentration.

2.6. Design of fixed bed

The various mathematical models have been developed for design of full-scale adsorption columns. In this study, six mathematical models were used for the design of the fixed bed columns from the collected experimental data as mentioned in Table 1.

2.7. Bed depth service time (BDST) model

The bed depth service time (BDST) model has been generally used for rapid prediction of adsorption column design and its performance is mentioned by Al-Degs et al. [33]. The BDST model generally predicts the relationship of bed depth (X) and service time (t) along with characteristic parameters like maximum adsorption capacity (No) and kinetic constant (K). The basic assumption of the BDST model states that the rate of adsorption is proportional to the residual capacity of adsorbent and to the concentration of the metal ion. The relation of service time with the process condition and operating parameters is represented in Eq. (1).

$$\ln\left(\frac{C_o}{C_b}-1\right)=\ln\left[\exp\left(\frac{KXN_o}{V}\right)-1\right]-KC_o t \quad (1)$$

The linear form of Bed-depth and service time is mentioned in Eq. (2).

$$t=\frac{N_o}{vC_o}X-\frac{1}{KC_o}\ln\left(\frac{C_o}{C_b}-1\right) \quad (2)$$

where C_o (mg/L) represents the influent metal ion concentration, C_b (mg/L) is the desired metal ion concentration at breakthrough time, K represents the adsorption rate constant (L/mg/h), N_o (mg/L) is the adsorption capacity, X represents the bed depth of column in (cm), v (cm/h) represents the linear flow velocity of feed to bed, and t (h) is the service time of the column under the above condition. The calculated value of N_o and K can be obtained from the slope (a) and intercept (b) of t vs. X plot. 7

2.8. Mass transfer model

The mass transfer kinetic model is given by Abia et al. [34]. The linear form of mass transfer kinetic model in Eq. (3).

$$\ln C_o - C_t = \ln D + K_o t \quad (3)$$

Table 1
Mathematical expression of adsorption column models

S. No.	Column models	Expression	References
1	Bed-depth and service time (BDST) model	$\ln\left(\frac{C_o}{C_b}-1\right)=\ln\left[\exp\left(\frac{KXN_o}{V}\right)-1\right]-KC_o t$	[26,27]
2	Mass transfer model	$C_o - C_t = D\exp(K_o t)$	[28,29]
3	Yoon nelson model	$\frac{C_e}{C_o}=\frac{1}{1+\exp[k(\tau - t)]}$	[30]
4	Thomas model	$\frac{C_t}{C_o}=\frac{1}{1+\exp\frac{K_T(q_m - C_o V)}{r}}$	[31,32]
5	Adam-Bohart model	$\ln\frac{C}{C_o}=kC_o t - kN_o\frac{z}{u}$	[33]
6	Wolborska model	$\ln\frac{C}{C_o}=\frac{\beta C_o}{N_o}t-\frac{\beta Z}{u}$	[33]

where C_o (mg/L) represents the influent metal ion concentration, C_t (mg/L) is the effluent metal ion concentration at shaking time (t) in min, D is the fitting parameter, K_o is the mass adsorption coefficient (min^{-1}). If the adsorption of the metal ion depicted by the mass transfer model then a plot of $\ln(C_\circ - C_t)$ vs. (t) should give a linear relationship. D and K_o can be determined from the intercept and slope of the plot respectively.

2.9. Yoon Nelson model

The assumption of Yoon and Nelson model predicted that the rate of probability to decrease in adsorption for each adsorbate molecule is proportional to the probability of adsorbate adsorption. For a single component system, the Yoon and Nelson model in Eq. (4) [35].

$$\frac{C_e}{C_o} = \frac{1}{1+\exp[k(\tau - t)]} \tag{4}$$

where C_o and C_e (mg/L) is the influent and effluent concentration respectively, k (l/min) represents the rate constant, τ represents the time (min) required for 50% adsorbate breakthrough and t represents breakthrough or sampling time in min.

2.10. Thomas model

This model has been widely used for finding the behavior of the adsorption process in a fixed bed column. The Thomas model is widely used in column performance modeling. Its derivation assumes Langmuir kinetics of adsorption-desorption and no axial dispersion. The Thomas model for adsorption column can be expressed in Eq. (5) [36].

$$\frac{C_t}{C_o} = \frac{1}{1+\exp\frac{K_T(q_m - C_o V)}{r}} \tag{5}$$

The linear form is expressed by Eq. (6).

$$\frac{K_T q_m}{r} - K_T C_o \frac{V}{r} = ln\frac{C_o - C_t}{C_t} \tag{6}$$

where slope "a" = $K_T\ C_o$, and intercept "b" = $K_T q_m/r$, C_o and C_t (mg/L) are the influent and effluent concentration respectively, K_T (L/min·mg) is the Thomas rate constant, q (mg/g) represents the maximum adsorption capacity, m (g) is the mass of adsorbent, V (ml) is the effluent volume and (r) represents the flow rate in (ml/min).

2.11. Adam-Bohart model

The Adams-Bohart model is based on the assumption that the rate of adsorption is proportional to both the concentration of the adsorbing species and the residual capacity of the adsorbent. This modal describes the relationship between C/C_o and time within an open system. The Adams-Bohart model is only used for the description of the initial part of the breakthrough curve represented by Eq. (7) [37].

$$\ln\frac{C}{C_o} = kC_o t - kN_o\frac{z}{u} \tag{7}$$

where C_o and C (mg/L) are the influent and effluent concentration respectively, z (cm) is the bed depth, u (cm/min) is the linear flow rate of metal ion solution, k (L/min·mg) is the adsorption rate constant and N_o (mg/L) is the saturation concentration.

2.12. Wolborska model

This model has been used for explaining the adsorption dynamics of the breakthrough curve. The mathematical expression of the Wolborska model is almost equivalent to the Adams- Bohart model represented by Eq. (8) [37].

$$\ln\frac{C}{C_o} = \frac{\beta C_o}{N_o}t - \frac{\beta Z}{u} \tag{8}$$

where β (min^{-1}) represents the kinetic coefficient of external mass transfer and remaining are same as in case of Adams-Bohart model.

3. Results and discussion

3.1. Characterization of natural biogenic iron oxide (BIF form) adsorbent

The EDS Spectra of BIF adsorbent represents the elemental composition in percentage of iron, silica, aluminium, oxygen and carbon etc before and after Cu(II) ion adsorption in column experiment. The EDS spectrum of BIF media before and after Cu(II) ion adsorption is shown in Figs. 1a and b.

The XRD analysis of BIF adsorbent before Cu(II) ion adsorption represent the presence of hematite (Fe_2O_3) at 2θ value 35.69° (referring JCPDS Card No.: 00-024-0072) along with aluminum oxide (Al_2O_3) at 58.96° (referring JCPDS Card No.: 75-0788), silicon dioxide (SiO2) at 49.51o (referring JCPDS Card No.:00-001-0378) [38]. The 2θ value 64.11° provides the presence of phosphorus pentaoxide (P_2O_5) (referring JCPDS Card No.: 23-1301), 2θ value 28.41° provides the presence of calcium carbonate ($CaCO_3$) (referring JCPDS Card No.: 04-011-3633) and magnesium oxide (MgO) at 39.63° (referring JCPDS Card No.: 02-1207) is shown in Fig. 2.

The FTIR spectrum of BIF adsorbent, before adsorption represents the Fe-O vibration mode of hematite (Fe_2O_3) in absorption bands range of 400–750 cm^{-1} as shown in Fig. 3a. The peaks at 474.78, 505.93, 675.86 cm^{-1} were due to the longitudinal absorption, at 580.96 cm^{-1} was due to the transverse absorption of hematite (Fe_2O_3) present in BIF adsorbent [39,40]. The absorption band of OH at vibrational modes 3403.54 cm^{-1} and 3685.84 cm^{-1}, C=O (keton) at 1726.34 cm^{-1}, $CONH_2$ (amide) at 1631.44 cm^{-1}, COOH (carboxylic group) at 1414.55 cm^{-1}, Si-O-Si and Si-O-C at 1028.96 cm^{-1}, C=C-H at 821.51 cm^{-1}, acetylene (C_2H_2) at 2128.31 cm^{-1}, C-H(-CH_2-, -CH_3) at 2920.35 cm^{-1} [41]. The FTIR of BIF adsorbent after Cu(II) ion adsorption representing two main vibrational modes for CuO observed at 468.72, and 544 cm^{-1} are shown in Fig. 3b. High frequency mode at 544 cm^{-1} was reported due to Cu-O vibration stretching [42]. The absorption band

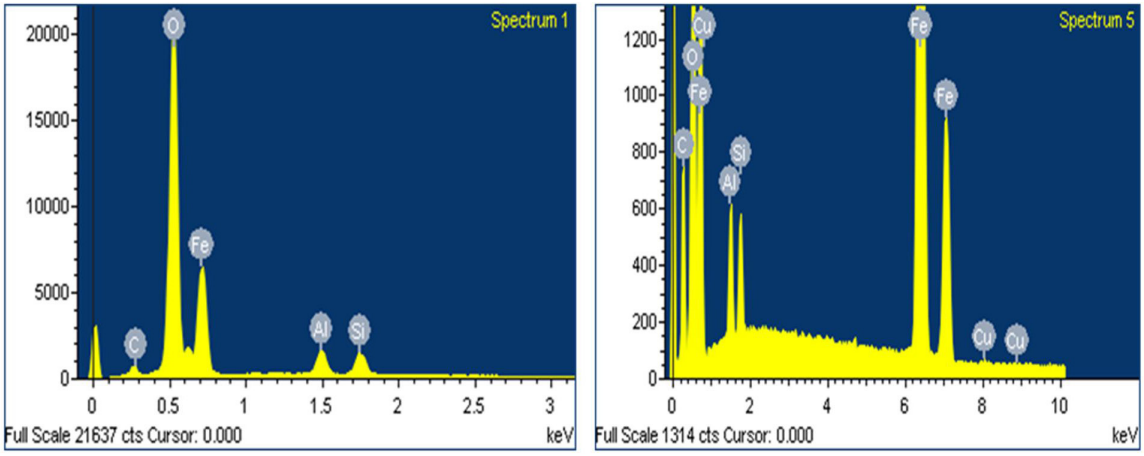

(a) Before Cu(II) ion adsorption (b) After Cu(II) ion adsorption

Fig. 1. EDS spectra of natural biogenic iron oxide (BIF form).

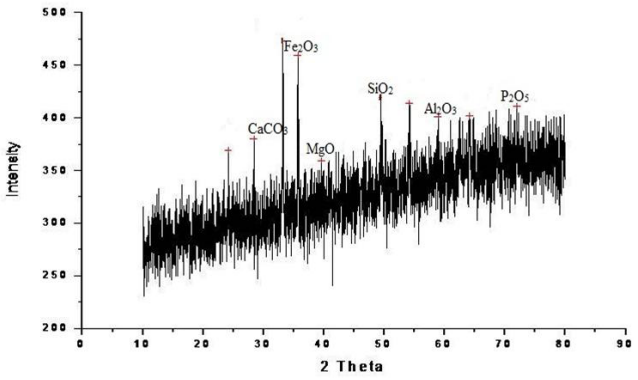

Fig. 2. XRD pattern of natural biogenic iron oxide (BIF form) adsorbent before Cu(II) ion adsorption.

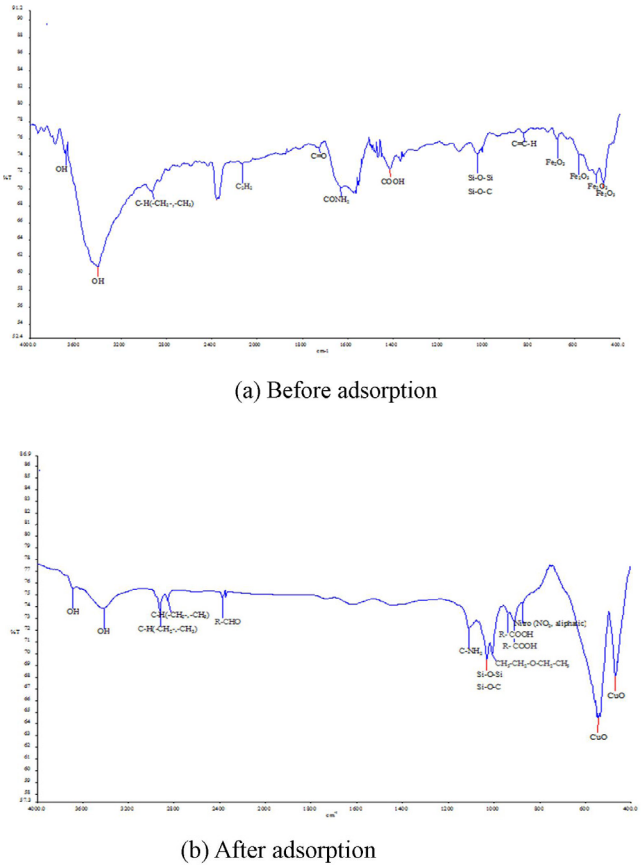

(a) Before adsorption

(b) After adsorption

Fig. 3. FTIR spectra of BIF adsorbent before and after Cu(II) ion adsorption.

of OH vibrational modes at 3687.91 cm^{-1} and 3415.38 cm^{-1} respectively; C-H(-CH_2-,-CH_3) vibrational modes at 2918.68 and 2852.74 cm^{-1} respectively; R-CHO (aldehyde) at 2373.63 cm^{-1}; Si-O-Si and Si-O-C at 1031.35 cm^{-1}; C-NH_2 at 1107.94 cm^{-1}; CH_3-CH_2-O-CH_2-CH_3 (ether) at 1007.12 cm^{-1}; carboxylic acid (R-COOH) vibrational modes at 912.87 and 939.17 cm^{-1} respectively; nitro (NO_2, aliphatic) at 873.42 cm^{-1}. The FTIR analysis of BIF adsorbent after Cu(II) ion adsorption shows the presence of CuO absorption band due to the Cu(II) ion adsorption that formed into oxide, and was not present in BIF adsorbent before adsorption and the similar results were also reported by Kishor and Rawal [31]. This studies revealed that Cu(II) ion adsorption has occurred onto BIF particle.

3.2. *Effect of varying flow rates*

The performance of natural biogenic iron oxide (BIF form) as an adsorbent in a column to remove Cu(II) ion from synthetic solution was analyzed at varying flow rates i.e., 0.283 $m^3/m^2/h$, 0.565 $m^3/m^2/h$ and 0.848 $m^3/m^2/h$. The influent concentration of Cu(II) ion synthetic solution was kept at 20 mg/L at pH 5 [43]. The bed depth of 75 µm size adsorbent media in column was kept at 10 cm. The effect of varying flow rates on the breakthrough curve is shown in Fig. 4. The service time and saturation time of the column were selected as the time when normalized con-

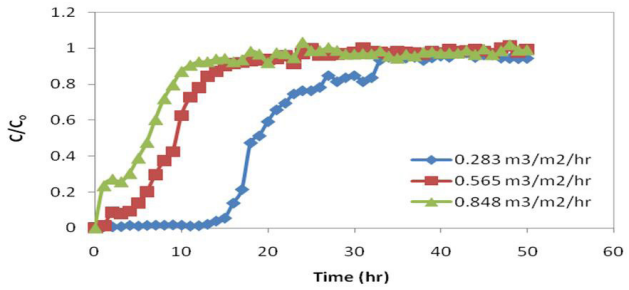

Fig. 4. Effect of varying flow rate variation on breakthrough curve.

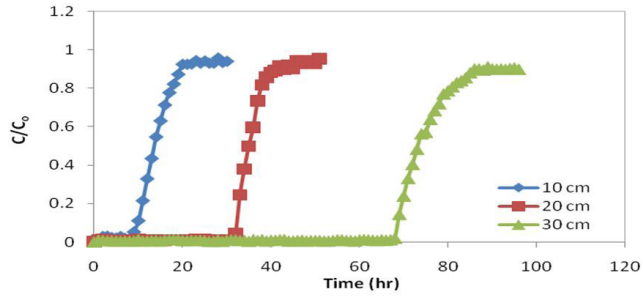

Fig. 5. Effect of varying bed depth on breakthrough curve.

centration C/C_o reached 0.05 and 0.90 respectively. It was found that 0.283 $m^3/m^2/h$ flow rate has maximum Cu(II) ion removal efficiency. The breakthrough time and exhaust time were achieved at 14 h (2.8 L) and 34 h (6.8 L) respectively. The breakthrough time decreased from 14 h (2.8 L) to 0 h (0 L) and exhaust time from 34 h (6.8 L) to 13 h (7.8 L) by increasing the flow rate from 0.283 $m^3/m^2/h$ to 0.848 $m^3/m^2/h$ respectively. It observed that the flow rate leads to a decrease in breakthrough time and adsorption capacity of the column. Similar results were also reported by Li et al. [44].

3.3. Effect of varying media bed depth

The performance of natural biogenic iron oxide (BIF form) as an adsorbent in adsorption was analyzed at varying media bed depths i.e., 10 cm, 20 cm and 30 cm with 75 µm size natural biogenic iron oxide (BIF form) as an adsorbent, the influent concentration was kept at 20 mg/L Cu(II) ion concentration at pH 5 and flow rate 0.283 $m^3/m^2/h$ respectively. The effect of varying bed depths on a breakthrough curve is shown in Fig. 5. It was observed that maximum Cu(II) ion removal efficiency was achieved at 30 cm as compared to 10 cm and 20 cm bed depth due to the large surface area available for adsorption process. The breakthrough time and exhaust time were obtained at 68 h (13.6 L) and 86 h (17.2 L) respectively. The breakthrough time increased from 9 h (1.8 L) to 68 h (13.6 L) and exhaust time from 20 h (4.0 L) to 86 h (17.2 L) by increasing the bed depth from 10 cm to 30 cm respectively. It observed that the breakthrough, as well as exhaustion time, extended with increasing with bed depth. It might because of the higher bed allowing the longer contact time for the media with metal ion concentration. The same pattern was also reported by Li et al. [44].

3.4. Effect of varying inlet Cu(II) ion concentration

The performance of natural biogenic iron oxide (BIF form) as an adsorbent in column study at varying Cu(II) ion concentration i.e., 20 mg/L, 30 mg/L and 40 mg/L for the removal Cu(II) ion synthetic solution were analyzed on 75 µm size of natural biogenic iron oxide (BIF form) as an adsorbent with 3.0 cm internal diameter of a column. The bed depth of media 30 cm, 5 pH and 0.283 $m^3/m^2/h$ flow rate was kept for Cu(II) ion synthetic solution. The effect of varying Cu(II) ion concentration on breakthrough curve

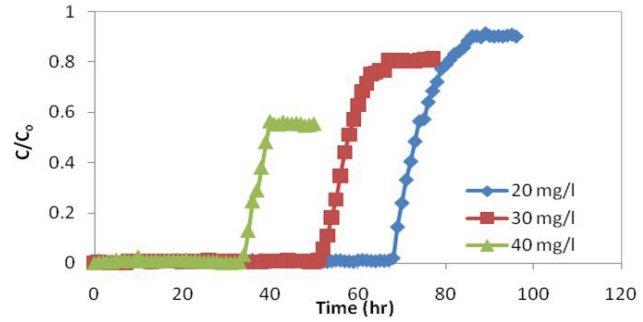

Fig. 6. Effect of varying initial Cu(II) ion concentration on breakthrough curve.

is shown in Fig. 6. The service time and saturation time of a column were selected as the time when normalized concentration C/C_o reached 0.05 and 0.90 respectively. It was observed from concentration study of column experiment that, maximum Cu(II) ion removal efficiency was achieved at 20 mg/L as compared to 30 mg/L and 40 mg/L initial Cu(II) ion concentration. The maximum breakthrough time and exhaust time at 20 mg/L initial Cu(II) ion concentration were achieved at 68 h (13.6 L) and 86 h (17.2 L) respectively. The breakthrough time decreased from 68 h (13.6 L) to 34 h (6.8 L) and exhaust time from 86 h (17.2 L) to 40 h (8.0 L) by increasing the initial Cu(II) ion concentration from 20 mg/L to 40 mg/L respectively. As the initial Cu(II) ion concentration was increased from 20 mg/L to 40 mg/L the breakthrough, exhaust time decreases for the treated volume (L) of Cu(II) ion synthetic solution. Similar results were also reported by Li et al. [44].

3.5. Mechanism of copper removal

The adsorption of metal ion on oxide surface involves the formation of bonds of the metal ion with the surface oxygen atoms and the release of protons from the surface equation:

$$= S - OH + M^{2+} \rightarrow = S - OM^{+} + H^{+} \quad (9)$$

where M^{2+} represents a divalent cation and S-OH represents an oxide surface.

At pH 5 some portion of solid Fe_2O_3 particle dissolves and reacts with aqueous Cu^{+2} ion to form CuO (s) and some Fe^{+3} in dissolved form.

pH 5

$$3\,Cu^{+2}(aq) + Fe_2O_3(s) \rightarrow 2\,Fe^{+3}(aq) + 3\,CuO(s) \quad (10)$$

The dissolved form of Fe^{+3} ions were passed through the effluent that resulted to decrease in (Fe) by weight percentage.

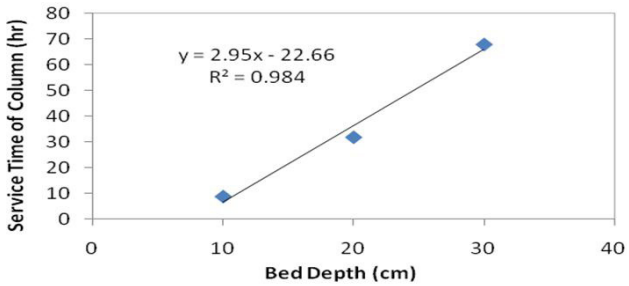

Fig. 7. BDST model at breakthrough time in fixed-bed column.

3.6. Evaluation of adsorption column design parameters

The modelling of the adsorption column was performed using column experiment data of different media bed depth study.

3.7. BDST model

The BDST model plot of service time (h) vs. bed depth (cm) for Cu(II) ion adsorption onto natural biogenic iron oxide (BIF form) as an adsorbent is shown in Fig. 7. The obtained data were fitted to the linear form of the BDST model and the parameters are presented in Table 2. BDST model predicted maximum adsorption potential and the data are best fitted in BDST model with high correlation coefficient (R^2) value of 0.984 suggesting that the bed depth (X) and service time (t) of a column show a linear relationship. The forces like intraparticle diffusion and external mass transfer resistance were negligible, hence Cu(II) ion get adsorbed onto the natural biogenic iron oxide (BIF form) surface directly. This model was best fit-

Table 2
Parameters of different models for adsorption of Cu(II) ion

BDST model					
Bed depth	No mg/l (adsorption capacity)	K_L mg^{-1} h^{-1} (adsorption rate constant)	R^2	Time of breakpoint (min)	
10–30 cm	1669.7	0.0064	0.984		
Yoon and Nelson model					
	k rate constant (min^{-1})	τ 50% Adsorbate breakthrough time (min)	R^2	Observed	Predicted
10 cm	0.005	941.2	0.91	540	361.3877
20 cm	0.003	2316.333	0.756	1920	1300.8415
30 cm	0.001	7136	0.659	4080	3244.1797
Mass transfer model					
Bed depth	K_o Mass transfer coefficient (min^{-1})	D (Fitting parameter)	R^2	Observed	Predicted
10 cm	–0.002	40.568	0.907	540	380.4397
20 cm	–0.001	47.56	0.704	1920	912.8353
30 cm	–0.000	37.75	0.581	4080	NA
Thomas model					
Bed depth	K_T L min^{-1} mg^{-1} (Thomas rate constant)	q mg/g (Maximum adsorption capacity)	R^2	Observed	Predicted
10 cm	0.0002	361.8664	0.91	540	361.3877
20 cm	0.0001	468.5830	0.756	1920	1301.8415
30 cm	0.0000	978.0327	0.659	4080	3244.1797
Adam-Bohart Model					
Bed depth	k_L/mg·min (Adsorption rate constant)	N_o mg/l (Saturation concentration)	R^2	Observed	Predicted
10 cm	0.0083	22.5755	0.799	9	6.2
20 cm	0.0060	23.6997	0.741	32	24.7
30 cm	0.003	34.0528	0.657	68	43.1
Wolborska Model					
Bed depth	β min^{-1} (Kinetic coefficient)	N_o mg/l (Saturation concentration)	R^2	Observed	Predicted
10 cm	0.1880	22.5191	0.799	9	6.2
20 cm	0.1434	23.6997	0.741	32	24.7
30 cm	0.1021	34.0528	0.657	68	43.1

ted which described the service time (h) and bed depth (cm) of the column.

3.8. Yoon and Nelson model

The Yoon and Nelson model for Cu(II) ion adsorption onto natural biogenic iron oxide (BIF form) as an adsorbent is shown in Fig. 8. The obtained data were fitted to Yoon and Nelson model and kinetic parameters are presented in Table 2. It can be observed that on increasing the media bed depth of a column the rate constant, k (min^{-1}) decreases and the predicted breakpoint time does not correspond and fit with the observed breakpoint time for 10 cm, 20 cm and 30 cm bed depth. Yoon and Nelson's model revealed that the decrease in probability rate of adsorption of each adsorbate molecule with respect to adsorbate adsorption and adsorbate breakthrough. The correlation coefficient (R^2) values were 0.91, 0.756 and 0.659 for 10 cm, 20 cm and 30 cm bed depth respectively. It is clearly observed that this model is not applicable and fit to describe the adsorption process and the rate of decrease in the probability of adsorption for each adsorbate molecule is proportional to the probability of adsorbate adsorption and adsorbate breakthrough on the adsorbent.

3.9. Mass transfer model

The mass transfer kinetic plot for Cu(II) ion adsorption onto natural biogenic iron oxide (BIF form) as an adsorbent is shown in Fig. 9. The obtained data were fitted to the mass transfer model and the kinetic parameters are presented in Table 2. The mass transfer model revealed that the plot of $\ln(C_o - C_t)$ vs. (t) should give a linear relationship. It can be observed that on increasing the media bed depth of a column the mass transfer coefficient, K_o (min^{-1}) increases negatively and the predicted breakpoint time does not correspond and fit with the observed breakpoint time for 10 cm, 20 cm and 30 cm bed depth. The correlation coefficient (R^2) values were 0.907, 0.704 and 0.581 for 10 cm, 20 cm, and 30 cm bed depth respectively revealed that this model is not applicable to describe the process.

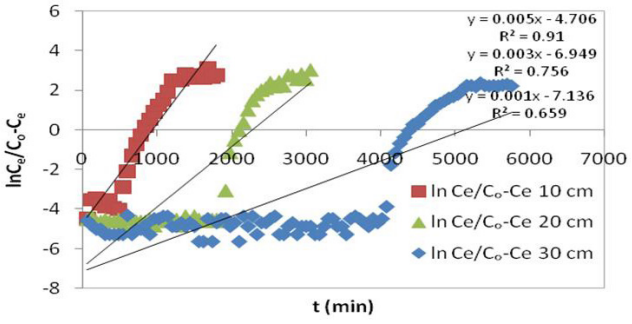

Fig. 8. Yoon and Nelson kinetic plot for the adsorption of Cu(II) ion.

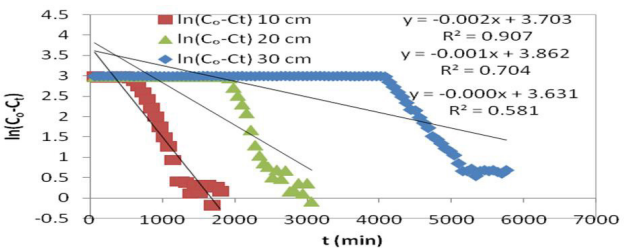

Fig. 9. Mass transfer kinetic plot for the adsorption of Cu(II) ion.

3.10. Thomas model

The Thomas model kinetic plot for Cu(II) ion adsorption onto natural biogenic iron oxide (BIF form) as an adsorbent is shown in Fig. 10. The kinetic parameters of the Thomas model are presented in Table 2. It is clearly observed that increasing the media bed depth of the column decreases the Thomas rate constant, K_T L/min·mg and increases the maximum adsorption capacity, q (mg/g). The predicted breakpoint time does not correspond and fit with the observed breakpoint time for 10 cm, 20 cm and 30 cm bed depth. The Thomas model revealed that behavior of adsorption process in fixed-bed column follows the Langmuir kinetics of sorption-desorption with no axial dispersion. The adsorption is not only limited by the chemical reaction but also controlled by the mass transfer at the interface and follows second order kinetics. The correlation coefficient (R^2) values for Thomas model were 0.91, 0.756 and 0.659 for 10 cm, 20 cm and 30 cm bed depth respectively and revealed that this model does not fit to describe the behaviour adsorption process in fixed bed column i.e. Cu(II) ion adsorption onto natural biogenic iron oxide (BIF form) adsorbent does not follow Langmuir kinetics of sorption-desorption with axial dispersion.

3.11. Adam-Bohart model

The Adam-Bohart model kinetic plot for Cu(II) ion adsorption onto natural biogenic iron oxide (BIF form) as adsorbent is shown in Fig. 11. The experimental data were fitted to Adam-Bohart model and the kinetic parameters are represented in Table 2. It is observed that with increasing the media bed depth of column the adsorption rate constant, k (L/min·mg) decreases and the saturation concentration, N_o (mg/L) increases. The predicted breakpoint time does not correspond and fit with the observed breakpoint time for 10 cm, 20 cm and 30 cm bed depth. Adams-Bohart model describes the relationship between C/C_o and time in

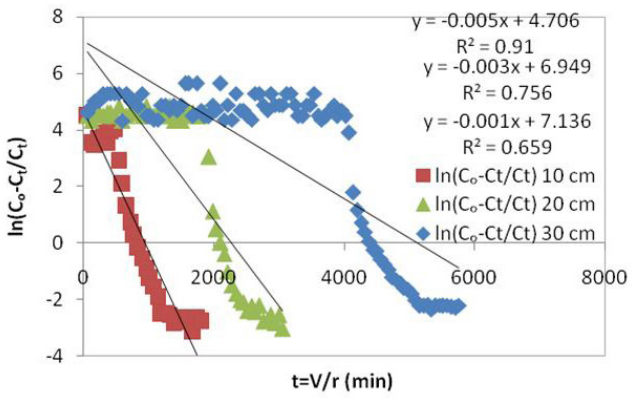

Fig. 10. Thomas model kinetic plot for the adsorption of Cu(II) ion.

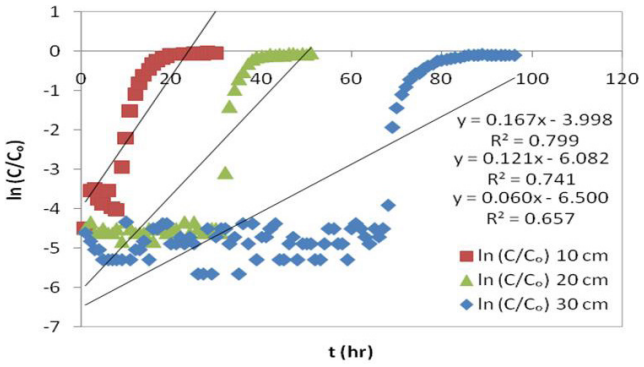

Fig. 11. Adam-Bohart model kinetic plot for the adsorption of Cu(II) ion.

the open system for the adsorption of the metal ion. The correlation coefficient (R^2) values for Adams-Bohart model were 0.799, 0.741 and 0.657 for 10 cm, 20 cm and 30 cm bed depth respectively which shown that this model is not fit to describe the relationship between C/C_o and time in fixed bed column for the adsorption of Cu(II) ion.

3.12. Wolborska model

The Wolborska model kinetic plot for Cu(II) ion adsorption onto natural biogenic iron oxide (BIF form) as adsorbent is shown in Fig. 12. The obtained data were fitted to Wolborska model and the kinetic parameters are presented in Table 2. It is observed that with increasing the media bed depth of a column the kinetic coefficient of external mass transfer β (min^{-1}) decreases and the saturation concentration N_o (mg/L) increases. The predicted breakpoint time does not correspond and fit with the observed breakpoint time for 10 cm, 20 cm and 30 cm bed depth. Wolborska model describes the adsorption dynamics in the low concentration range of the breakthrough curve. The correlation coefficient (R^2) values were 0.799, 0.741 and 0.657 for 10 cm, 20 cm and 30 cm bed depth respectively which shown that this model is not applicable to describe that the adsorption dynamics is in the low concentration range of the breakthrough curve in fixed bed column.

As shown in Table 2, the data best fitted with high correlation coefficient (R^2) value 0.984 of BDST model describe the linear relationship of bed depth (X) and service time (t) of the column with respect to other models. The poorly fitted in Thomas model, Yoon-Nelson model, mass transfer model, Adam-Bohart model, Wolborska model.

4. Conclusion

The natural biogenic iron oxide (BIF form) is naturally occurring highly rich iron oxide ores available in huge quantity in the mines. The adsorbent media was prepared from ores and tested for the removal of Cu(II) ion from synthetic wastewater in column experiments. The breakthrough time was achieved at 14 h and exhaust/saturation point was achieved at 34 h at 0.283 $m^3/m^2/h$ as compared to $m^3/m^2/h$ and 0.848 $m^3/m^2/h$ flow rate without leaching of minerals during the column operation. The FTIR analysis of BIF

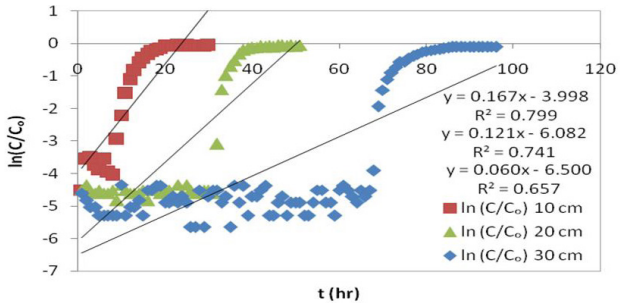

Fig. 12. Wolborska model kinetic plot for the adsorption of Cu(II) ion.

adsorbent after Cu(II) ion adsorption shows the presence of CuO absorption band due to the Cu(II) ion adsorption that formed into oxide, and was not present in BIF adsorbent before adsorption. The BDST adsorption modal predicted to best describe the adsorption kinetics with a high correlation coefficient (R^2) value of 0.984 with experimental data, and poorly fitted in Thomas model, Yoon-Nelson model, mass transfer model, Adam-Bohart model and Wolborska model. This study suggests that low cost natural biogenic iron oxide (BIF form) may be used as a viable and sustainable adsorbent for copper (II) metal ion removal from water and industrial wastewaters.

References

[1] R.S. Juang,H.J. Shao, Effect of pH on competitive adsorption of Cu(II), Ni(II), and Zn(II) from water onto chitosan beads, Adsorption 8 (2002) 71.
[2] W.S.W. Ngah, A. Kamari, Y.J. Koay, Equilibrium and kinetics studies of adsorption of copper (II) on chitosan and chitosan/PVA beads, Int. J. Biol. Macromol., 34 (2004) 155–163.
[3] J.W. Patterson, Industrial wastewater treatment technology, 2nd ed., Stoneham, MA: Butterworths Publishers, (1985).
[4] C.R. Krishnamurthy, P. Vishwanathan, Toxic metals in the Indian environment. Tata Mc Graw Hill Publishing Company Limited, New Delhi, 1991, 188 p.
[5] R. Katal, H. Zare, S.O. Rastegar, P.G. Mavaddat, N. Darzi, Removal of dye and chemical oxygen demand reduction from textile industrial wastewater using hybrid bioreactors, Environ. Eng. Manag. J., 13 (2014) 43–50.
[6] S.I. Siddiqui, S.A. Chaudhry, Iron oxide and its modified forms as an adsorbent for arsenic removal: a comprehensive recent advancement, Process. Saf. Environ. Prot., 111 (2017) 592–626.
[7] S.I. Siddiqui, S.A. Chaudhry, Arsenic removal from water using nanocomposite: a review, Curr. Environ. Eng., 4 (2017) 81–102.
[8] S.H. Siddiqui, The removal of Cu^{2+}, Ni^{2+} and methylene blue (MB) from aqueous solution using Luffa Actangula carbon: kinetics, thermodynamic and isotherm and response methodology, Groundwater Sustain. Dev., 6 (2018) 141–149.
[9] S.I. Siddiqui, S.A. Chaudhry, S.U. Islam, Green adsorbents from plant sources for the removal of arsenic: an emerging wastewater treatment technology, in: S.U. Islam (Ed.), Plant-based Natural Products: Derivatives and Applications, John Wiley & Sons, Inc., 2017
[10] S.I. Siddiqui, G. Rathi, S.A. Chaudhry, Acid washed black cumin seed powder preparation for adsorption of methylene blue dye from aqueous solution: Thermodynamic, kinetic and isotherm studies, J. Molec. Liq., 264 (2018) 275–284
[11] N. Rawal, U. Jarouliya, Removal of chromium (VI) ions from wastewaters by low cost adsorbent, Res. J. Chem. Environ., 17 (2013) 43–47.

[12] A.A. Alqadami, M. Naushad, Z.A. Alothman, A.A. Ghfar, Novel metal organic framework (MOF) based composite material for the sequestration of U(VI) and Th(IV) metal ions from aqueous environment RSC Adv., 6(27) (2016) 22679–22689.
[13] A.A. Alqadami, M. Naushad, M.A. Abdalla, T. Ahamad, Z. Abdullah Alothman, S.M. Alshehri, Synthesis and characterization of Fe_3O_4@TSC nanocomposite: highly efficient removal of toxic metal ions from aqueous medium, RSC Adv., 6 (2016) 22679–22689.
[14] H.J. Shipley, K.E. Engates, V.A. Grover, Removal of Pb(II), Cd(II), Cu(II), and Zn(II) by hematite nanoparticles: effect of sorbent concentration, pH, temperature, and exhaustion, Environ. Sci. Pollut. Res., 20 (2013) 1727–1736.
[15] M. Kremplova, D. Fialova, D. Hynek, V. Adam, R. Kizek, Utilization of the iron nanoparticles for heavy metal removal from the environment, Mendelnet, (2013) 924–928.
[16] M. Sukopova, J. Matysikova, O. Skorvan, M. Holba, Application of iron nanoparticles for industrial wastewater treatment, Nanocon, 16–18. Oct., Brno, Czech Republic, EU (2013).
[17] N. Sezgin, M. Sahin, A. Yalcin, Y. Koseoglu, Synthesis characterization and the heavy metal removal efficiency of MFe_2O_4 (M=Ni, Cu) Nanoparticles, Ekoloji, 22 (2013) 89–96.
[18] A.B. Seabra, P. Haddad, N. Duran, Biogenic synthesis of nanostructured iron compounds: application and perspectives, IET Nanobiotechnol., 7 (2013) 90–99.
[19] H. Katerina, S. Ivo, F. Jan, N. Maryla, T. Jiri, S. Mirka, H. Hideki, T. Jun, Z. Radek, Magnetically responsive natural biogenic iron oxides for organic xenobiotics removal, Nanocon, 16–18 Oct., Brno, Czech Republic, EU (2013).
[20] E.O. Omoregie, R.M. Couture, P.V. Cappellen, C.L. Corkhill, J.M. Charnock, D.A. Polya, D. Vaughan, K. Vanbroekhoven, J.R. Lloyd, Arsenic bioremediation by biogenic iron oxides and sulphides, Appl. Environ. Microbiol., 79 (2013) 432–4335.
[21] A.J. Williams, D.Y. Sumner, C.N. Alpers, K.M. Campbell, D.K. Nordstrom, Biogenic iron mineralization at iron mountain, ca, with implication for detection with the mars curiosity rover, 45th Lunar and Planetary Science Conference (2014).
[22] J.A. Rentz, J.L. Ullman, Copper and zinc removal using biogenic iron oxides, World Environ. Water Res. Congress: Crossing Boundaries (2012).
[23] G.M. Ayoub, H. Kalinian, Removal of low-concentration phosphorus using a fluidized raw dolomite bed, Water Env. Res., 78 (2006) 353–361.
[24] P. Cloud, Paleoecological significance of the banded iron formation, Econ. Geol., 68 (1973) 1135–1143.
[25] S.S. Goldich, Ages of Precambrian banded iron-formation, Econ. Geol., 68 (1973) 1126–1134.
[26] D. Emerson, N.P. Revsbech, Investigation of an iron-oxidizing microbial mat community located near Aarhus, Denmark: field studies, Appl. Environ. Microbiol., 60 (1994) 4022–4031.
[27] D. Emerson, C. Moyer, Isolation and characterization of novel iron-oxidizing bacteria that grow at circumneutral pH, Appl. Environ. Microbiol., 63 (1997) 4784–4792.
[28] D. Fortin, S. Langley, Formation and occurrence of biogenic iron-rich minerals, Earth-Sci. Rev., 72 (2005) 1–19.
[29] D.E. Weiss, Bacterial iron oxidation in circumneutral freshwater habitats: findings from the field and the laboratory, Geomicro. J., 21 (2004) 405–414.
[30] K.J. Edwards, W. Bach, T.M. McCollom, D.R. Rogers, Neutrophilic iron-oxidizing bacteria in the ocean: Their habitats, diversity, and roles in mineral deposition, rock alteration, and biomass production in the deep-sea, Geomicro. J., 21 (2004) 393–404.
[31] B. Kishor, N.R. Rawal, Studies on natural biogenic iron oxides for removal of copper (II) ion from aqueous solution, Desal. Water Treat., 88 (2017) 145–153.
[32] APHA, Standard methods for the examination of water and wastewater 22rd edition. American Public Health Association, American Water Works Association, Water Environment Federation, 2012.
[33] Y.S. Al-Degs, M.A.M. Khraisheh, S.J. Allen, M.N. Ahmad, Adsorption characteristics of reactive dyes in columns of activated carbon, J. Hazard. Mater., 165 (2009) 944–949.
[34] A.A. Abia, O.B. Didi, E.D. Asuquo, Modelling of Cd(II) sorption kinetics from aqueous solution onto some Thiolated agricultural waste adsorbents, J. Appl. Sci. 6(12) (2006) 2549–2556.
[35] J.T. Nwabanne, P.K. Igbokwe, Adsorption performance of packed bed column for the removal of lead (II) using oil palm fibre, Int. J. Appl. Sci. Technol., 2(5) (2012) 148–156.
[36] K.S. Bharathi, S.P.T. Ramesh, Fixed-bed column studies on biosorption of crystal violet from aqueous solution by citrullus lanatus rind and cyperus rotundus, Appl. Water Sci., 3 (2013) 673–687.
[37] A. Saravanan, N. Uvaraja, S. Krishnan, Column study on the removal of metals from industrial effluents using the biomass sargassum sp., Int. J. Appl. Res. Mech. Eng. (IJARME), 2(1) (2012) 135–145.
[38] B.H. Stuart, Infrared Spectroscopy: Fundamentals and Applications, Wiley, UK, 2004, 143 p.
[39] M. Naushad, T. Ahamad, G. Sharma, H. Ala'a, A.B. Albadarin, M.M. Alam, Z.A. ALOthman, S.M. Alshehri, A.A. Ghfar, Synthesis and characterization of a new starch/SnO_2 nanocomposite for efficient adsorption of toxic Hg^{2+} metal ion, Chem. Eng. J., 300 (2016) 306–316.
[40] M. Naushad, T. Ahamad, B.M. Al-Maswari, A. Abdullah Alqadami, S.M. Alshehri, Nickel ferrite bearing nitrogen-doped mesoporous carbon as efficient adsorbent for the removal of highly toxic metal ion from aqueous medium, Chem. Eng. J., 330 (2017) 1351–1360.
[41] N.E.A. El-Gamela, L. Wortmann, K. Arroubb, S. Mathur, Surface immobilization and release of sparfloxacin drug from SiO_2@Fe_2O_3 core-shell nanoparticles, Electro. Supple. Mater. (ESI) for chemical communications, Royal Soc. Chem., (2011).
[42] R.D. Braun, Introduction to Instrumental Analysis, McGraw-Hil, Chemistry series. 1987, pp. 378–379.
[43] M.R. Awual, G.E. Eldesoky, T. Yaita, M. Naushad, H. Shiwaku, Z.A. AlOthman, S. Suzuki, Schiff based ligand containing nano-composite adsorbent for optical copper(II) ions removal from aqueous solutions, Chem. Eng. J., 279 (2015) 639–647.
[44] N. Li, J. Ren, L. Zhao, Z.L. Wang, Fixed bed adsorption study on phosphate removal using nanosized FeOOH-modified anion resin, J. Nanomater., Hindawi Publishing Corporation, (2013) (736275) (2013) 5–13.